ORIGINAL ARTICLE

TTC5 syndrome: Clinical and molecular spectrum of a severe and recognizable condition

Luciana Musante[1] | Flavio Faletra[1] | Kolja Meier[2] | Hoda Tomoum[3] |
Paria Najarzadeh Torbati[4] | Edward Blair[5] | Sally North[5] | Jutta Gärtner[2] |
Susann Diegmann[2] | Mehran Beiraghi Toosi[6] | Farah Ashrafzadeh[7] |
Ehsan Ghayoor Karimiani[4,8,9] | David Murphy[10] | Flora Maria Murru[1] |
Caterina Zanus[1] | Andrea Magnolato[1] | Martina La Bianca[1] |
Agnese Feresin[11] | Giorgia Girotto[1,11] | Paolo Gasparini[1,11] |
Paola Costa[1] | Marco Carrozzi[1]

[1]Institute for Maternal and Child Health - IRCCS "Burlo Garofolo", Trieste, Italy

[2]Department of Pediatrics and Adolescent Medicine, University Medical Center Göttingen, Göttingen, Germany

[3]Department of Pediatrics, Ain Shams University, Cairo, Egypt

[4]Department of Molecular Genetics, Next Generation Genetic Polyclinic, Mashhad, Iran

[5]Oxford Centre for Genomic Medicine, Oxford University Hospitals NHS Foundation Trust, Oxford, UK

[6]Pediatric Neurology Department, Ghaem Hospital, Mashhad University of Medical Sciences, Mashhad, Iran

[7]Department of Pediatrics, Faculty of Medicine, Mashhad University of Medical Sciences, Mashhad, Iran

[8]Molecular and Clinical Sciences Institute, St. George's, University of London, London, UK

[9]Innovative Medical Research Center, Mashhad Branch, Islamic Azad University, Mashhad, Iran

[10]Department of Clinical and Movement Neurosciences, UCL Queen Square Institute of Neurology, University College London, London, UK

[11]Department of Medical, Surgical and Health Sciences, University of Trieste, Trieste, Italy

Correspondence
Luciana Musante, S.C. Genetica Medica, IRCCS Burlo Garofolo, Via dell'Istria 65/1, 34137 Trieste, Italy.
Email: luciana.musante@burlo.trieste.it

Abstract

Biallelic mutations in the *TTC5* gene have been associated with autosomal recessive intellectual disability (ARID) and subsequently with an ID syndrome including severe speech impairment, cerebral atrophy, and hypotonia as clinical cornerstones. A *TTC5* role in IDs has been proposed based on the physical interaction of TTC5 with p300, and possibly reducing p300 co-activator complex activity, similarly to what was observed in Menke-Hennekam 1 and 2 patients (MKHK1 and 2) carrying, respectively, mutations in exon 30 and 31 of *CREBBP* and *EP300*, which code for the TTC5-binding region. Recently, *TTC5*-related brain malformation has been linked to tubulinopathies due to the function of TTC5 in tubulins' dynamics. We reported seven new patients with novel or recurrent *TTC5* variants. The deep characterization of the molecular and phenotypic spectrum confirmed *TTC5*-related disorder as a recognizable, very severe neurodevelopmental syndrome. In addition, other relevant

clinical aspects, including a severe pre- and postnatal growth retardation, cryptorchidism, and epilepsy, have emerged from the reversal phenotype approach and the review of already published *TTC5* cases. Microcephaly and facial dysmorphism resulted in being less variable than that documented before. The *TTC5* clinical features have been compared with MKHK1 published cases in the hypothesis that clinical overlap in some characteristics of the two conditions was related to the common p300 molecular pathway.

KEYWORDS
biallelic mutations, deep phenotyping, severe NDD syndrome, *TTC5*

1 | INTRODUCTION

Neurodevelopmental disorders (NDDs) are complex and highly heterogeneous conditions; they often show overlapping characteristics and share a spectrum of disease-associated genes, thus raising unexpected difficulties and new challenges to the traditional syndrome-based approach. For this reason, thanks to the continuous advancement of NGS (next-generation sequencing) technologies, the characteristics delineation of a specific syndrome often follows the genetic results by describing patients' recurrent clinical features that share the same molecular defect. This approach, called reverse phenotyping, is a highly effective and valuable strategy for obtaining information on the gene-specific phenotypic spectrum (de Goede et al., 2016; Stessman et al., 2017; Uliana & Percesepe, 2016), remarking that pathogenic variants in a gene, initially considered the cause of a specific symptom (i.e., intellectual disability or epilepsy), then found to be associate with a broad neurodevelopmental phenotype (Abramov et al., 2021; Weng et al., 2021).

However, hypothesizing a syndrome starting from recognized descriptive clinical criteria allows the clinician to suspect a genetic diagnosis and guide geneticists to choose the technique with the higher diagnostic yield, which is more effective economically and time-saving. Lastly, reverse phenotyping can support molecular findings, confirming the initial hypothesis and establishing the causality of novel or uncertain results (Vulto-van Silfhout et al., 2017). The tetratricopeptide repeat domain-containing protein 5 gene (*TTC5*) encodes a stress-inducible transcription cofactor that interacts with lysine acetyltransferase p300 and several components of the p300 complex in the nucleus (Demonacos et al., 2001). p300 and its paralog CREB-binding protein are involved in histone acetylation and chromatin remodeling, thereby regulating several cellular processes such as proliferation, transformation, apoptosis, inflammation, and metabolism (Davies et al., 2011; Xiong et al., 2013) and have a crucial role in neuronal plasticity and cognition (Van Gils et al., 2021). Heterozygous mutations in *EP300* and *CREBBP* are considered the cause of the Rubinstein-Taybi syndrome (RSTS) (MIM:#180849; #613684). Deep phenotyping analysis shows that missense variants in exons 30 and 31 of *CREBBP* and *EP300*, which code for the TTC5-binding region, result in a diverse clinical phenotype the Menke-Hennekam syndrome

1 and 2 (MKHK1, MIM: #618332; MKHK2, MIM: #618333; Menke et al., 2016, 2018; Van Gils et al., 2021).

Despite its localization in the nucleus, TTC5 is also found in the cytosol, identified as a tubulin-specific ribosome-associating factor driving the co-translational degradation of tubulin mRNA when soluble α/β-tubulin concentration increases in the cells (Lin et al., 2020). A dynamic equilibrium between the polymerized and depolymerized (soluble) forms of tubulin is critical for cell division, intracellular trafficking, cell shape, and neuronal morphology (Dent, 2017; Saunders et al., 2022). Mutations in tubulin genes are responsible for a large spectrum of brain malformations such as abnormal neuronal migration and organization, differentiation, and axon guidance, with motor impairment, intellectual disability, and epilepsy being the main clinical symptoms (Romaniello et al., 2019).

In 2019, homozygous mutations in *TTC5* were associated with autosomal recessive intellectual disability (ARID) in two families (Hu et al., 2019). Subsequently, Rasheed and colleagues defined an intellectual disability syndrome reporting eight patients with severe speech impairment, cerebral atrophy, and hypotonia as clinical milestones (Rasheed et al., 2021). The authors hypothesized a role of TTC5 in IDs, based on the physical interaction of TTC5 with p300, mutated in RSTS and MKHK patients. In 2021, Miyamoto described a Japanese boy with *TTC5* compound heterozygous variants providing a detailed neuroradiological description and functional data and suggesting a link between *TTC5*-related brain malformation and the tubulinopathies (Miyamoto et al., 2021).

Our article delineates the phenotype of seven new *TTC5* cases with novel or recurrent mutations from five unrelated families; six of the probands present with homozygous variants, and one, born from non-consanguineous parents, with compound heterozygous variants in the *TTC5* gene.

The study aimed to (1) strengthen the clinical and genetic definition of a TTC5-related neurodevelopmental syndrome, confirming the milestone features already proposed to prioritize this syndrome for diagnosis; (2) highlight some emerging clinical aspects, including the severity of the impairment of motor and language functions, the severe pre and postnatal growth retardation, cryptorchidism and the presence of epilepsy; (3) provide a comprehensive phenotype description of *TTC5*-patients and compare it with the MKHK1, a recognizable

syndrome different from RSTS, caused by variants in exons 30 and 31 of *CREBBP*, to investigate the consistency of some observed clinical overlapping features; and (4) underline the importance of the deep reversal phenotype approach for interpreting molecular data.

2 | MATERIALS AND METHODS

Investigations were conducted in accordance with the ethical standards of the appropriate local Institutional Ethical Committees. Informed consent from the participating subjects was collected.

The multicentric, retrospective study enrolled seven patients from five unrelated families (Figure 1) with a severe NDD.

Patient 1 was recruited in the Neuropediatric Department of the IRCCS Burlo Garofolo in Trieste, Italy. We used GeneMatcher (patients 2–6; Sobreira et al., 2015) and data from the Deciphering Developmental Disorders (DDD) Study via DECIPHER (patient 7; Firth et al., 2011) to enlist a cohort of seven individuals. Probands were investigated by their referred physicians. The clinical information was standardized using the Human Phenotype Ontology (HPO; Köhler et al., 2021) to allow a reliable comparison of clinical features among individuals.

According to standard procedures, genomic DNA was extracted from patients' and parents' venous peripheral blood lymphocytes.

WES analysis was performed on the trio (patient and both parents) unless differently indicated.

Target enrichment kits, WES statistics and predicted functional impact, based on ACMG guidelines (Richards et al., 2015) and Varsome (https://varsome.com), are reported in Table S1.

In detail: WES analysis of patient 1, born from non-consanguineous parents, was performed at the IRCCS Burlo Garofolo (Trieste, Italy). According to the manufacturer, DNA was processed for library enrichment with the Twist Human Core for Enrichment-Exome panel (Twist). Sequencing was performed on NextSeq 500 (Illumina, San Diego, CA) instrument. Sequencing reads were aligned to the human reference genome (GRCh37/hg19) employing the BWA-mem tool, and variant calling were performed with GATK v4.1.2 HaplotypeCaller (EnGenome, Pavia, Italy). Annotation and prioritization of the variants were conducted with eVAI-enGenome software based on the American College of Medical Genetics and Genomics (ACMG) guidelines (Richards et al., 2015). SNVs and INDELs were filtered referring to public databases (dbSNP build150, NHLBI Exome Sequencing Project (ESP), Exome Aggregation Consortium (ExAC) database, Genome Aggregation Database (gnomAD)) and led to ruling out those variants previously reported as polymorphism. In particular, a minor allele frequency (MAF) cut-off of ≤0.01% was utilized. The trio was examined for the following inheritance patterns: de novo, homozygous recessive, compound heterozygous, and hemizygous. The pathogenicity of variants was assessed with the ClinVar, The Human Gene Mutation Database (HGMD), Online Mendelian Inheritance in Man (OMIM), and DECIPHER. Several in silico tools, such as PolyPhen-2 (Adzhubei et al., 2013), Sorting Intolerant from Tolerant (SIFT) (Sim et al., 2012), PaPI (Limongelli et al., 2015), DANN (Quang et al., 2015), dbscSNV score (Jian et al., 2014), and Combined Annotation Dependent Depletion (CADD) score (Kircher et al., 2014), were applied to establish the pathogenicity of novel variants. The diagnostic procedure adopted included discussion of WES data in
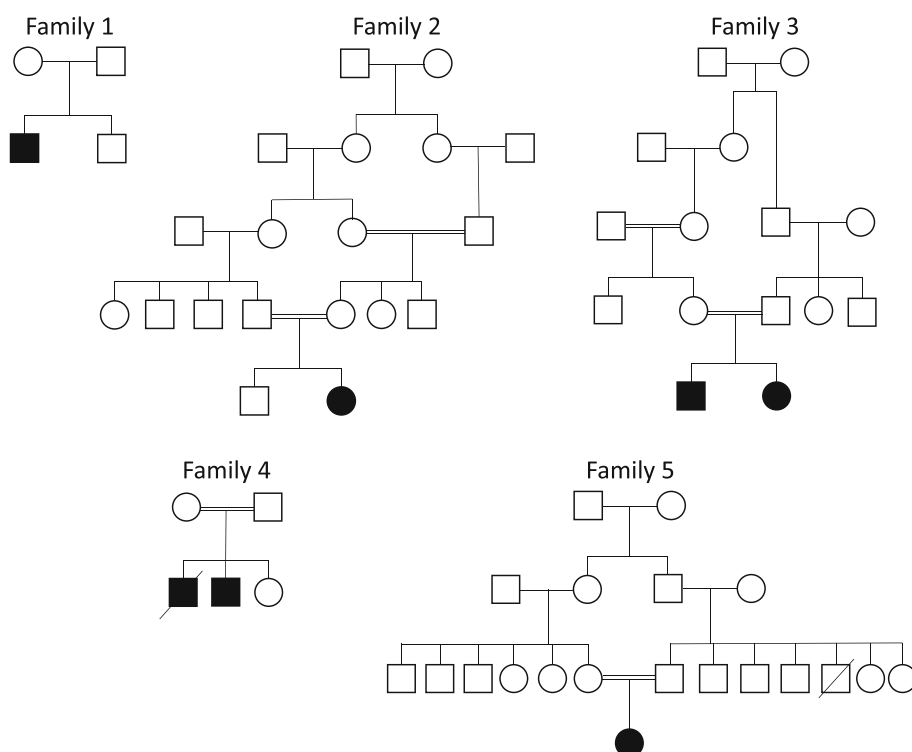
FIGURE 1 Pedigrees of the five unrelated families included in the study. Double bar, parental consanguinity; square, male; circle, female; filled, affected; unfilled unaffected; backslash, deceased

the context of phenotypic data at interdisciplinary meetings; the interpretation of WES data was supported by systematic bibliographic review and public database consultation (Musante et al., 2022). Variants' validation and segregation analyses were carried out by Sanger sequencing. Exome sequencing of patient 2 was performed at UCL Institute of Neurology and patient 3 (sequenced in single) at Centogene AG (Rostock, Germany). WES methods and data processing, including sequence alignment to GRCh37/GRCh38, variant filtering and prioritization by allele frequency, predicted functional impact, inheritance, and validation, were performed as previously reported (Bauer et al., 2019; Efthymiou et al., 2021).

WES analysis of patient 7 has been executed in the frame of the DDD study; methods and data processing, including variant filtering and prioritization, were performed as previously reported (Deciphering Developmental Disorders Study, 2017).

Exome sequencing of patients 5 and 6 was performed using SureSelect Human All Exon V6 enrichment kit (Agilent) and a HiSeq4000 sequencer (Illumina) at the Cologne Center for Genomics (CCG,

University of Cologne, Germany). The data were analyzed with the Varbank 2 pipeline (https://varbank.ccg.uni-koeln.de/varbank2, version 3.4), and categorization was based on ACMG guidelines 2015. Rare (MAF ≤0.001 in gnomAD) missense, INDEL, and intron variants with splice site effects were filtered for high quality. Pipeline-related false positives and recurrent variants biologically/clinically irrelevant were further reduced by utilizing an in-house database. Compound heterozygous and homozygous variants present in both brothers were considered for further analysis. Variants' validation and segregation analyses were carried out by Sanger sequencing.

3 | RESULTS

3.1 | Molecular findings

All novel and recurrent *TTC5* variants identified in this study are reported in Figure 2 and Table 1.
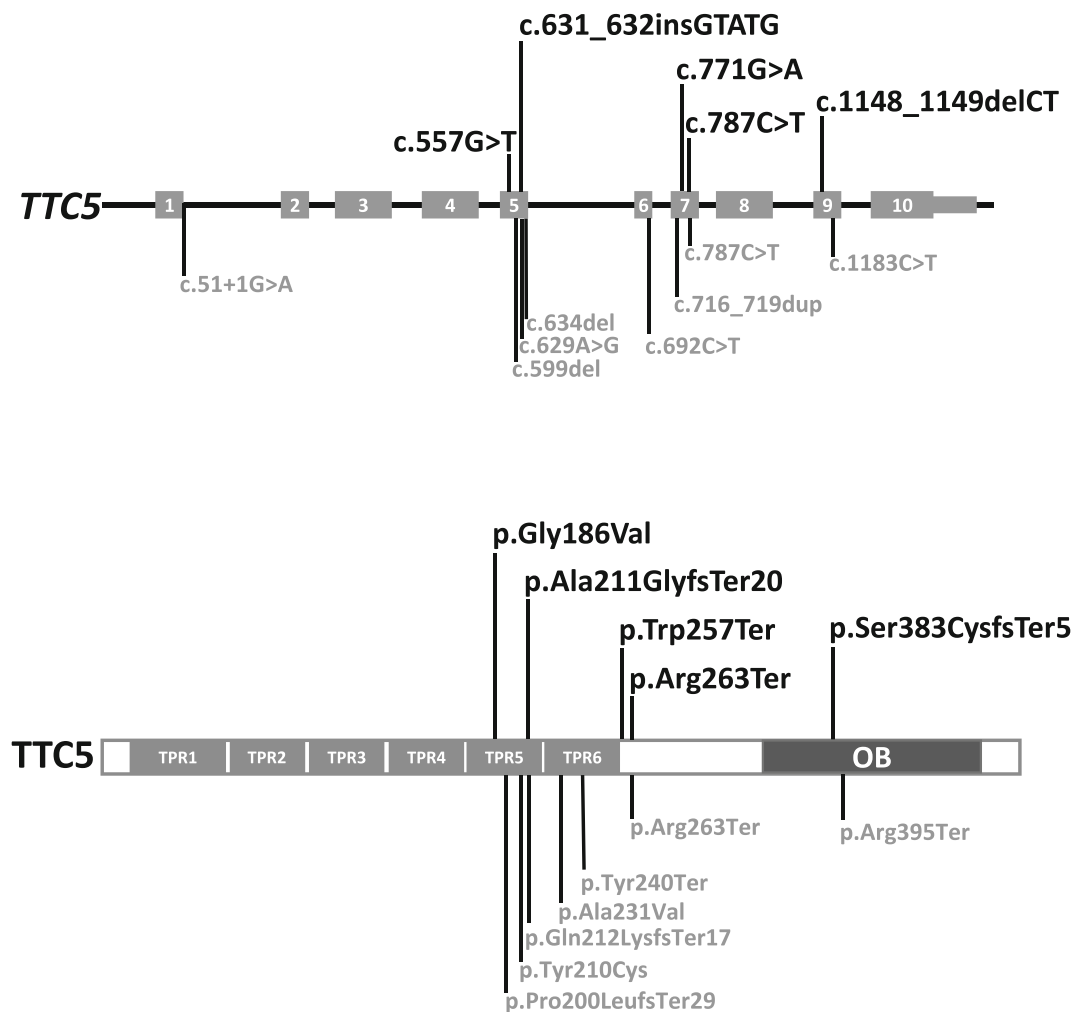
FIGURE 2 Schematic representation of *TTC5* gene and protein. Type and location of *TTC5* mutations identified in the patients reported in this study (black and bold) and previously published in the literature (gray) (Hu et al., 2019; Miyamoto et al., 2021; Rasheed et al., 2021). The position of the variants along the *TTC5* gene, as well as the position of the corresponding protein changes, is indicated. The shown tetratricopeptide domains (TPR 1–6) and oligonucleotide binding domain (OB) are based on UniProtKB/Swiss-Prot entry Q8N0Z6

TABLE 1 Summary of TTC5 genetic findings in the patients included in this study

	Family 1	Family 2	Family 3	Family 3	Family 4	Family 4	Family 5
Patient	1	2	3	4	5	6	7
Gender	M	F	M	F	M	M	F
Ethnicity	Italian	Iranian	Egyptian	Egyptian	Turkish	Turkish	Pakistani
Consanguinity	−	+	+	+	+	+	+
TTC5 variant NM_138376.2	c.557G>T c.1148_1149delCT	c.771G>A	c.787C>T	c.787C>T	c.631_632insGTATG	c.631_632insGTATG	c.787C>T
Predicted protein change	p.Gly186Val p.Ser383CysfsTer5	p.Trp257Ter	p.Arg263Ter	p.Arg263Ter	p.Ala211GlyfsTer20	p.Ala211GlyfsTer20	p.Arg263Ter
Exon	5 and 9	7	7	7	5	6	7
Variant type	Novel compound heterozygous	Novel homozygous	Recurrent homozygous	Recurrent homozygous	Novel homozygous	Novel homozygous	Recurrent homozygous

WES analysis on patient 1 revealed a compound heterozygous genotype of the *TTC5* gene, including a deletion of two bases in exon 9 (NM_138376.2: c.1148_1149delCT, p.Ser383CysfsTer5) inherited from the healthy father, leading to a premature stop codon (Figure 2), predicted to be pathogenic according to the ACMG guidelines and Varsome (Table S1). Given its position relative to terminal exon 10, it is likely to cause nonsense-mediated decay (NMD), resulting in the complete loss of a functional gene product from this allele. The second change altered a highly conserved nucleotide, located in exon 5 (NM_138376.2: c.557G>T, p.Gly186Val; Figure 2), inherited from the unaffected mother. It was predicted to be VUS-likely pathogenic according to the ACMG guidelines and Varsome (Table S1) and pathogenetic by the tools used during the analysis (PaPI score, Polyphen, SIFT, DANN score) and with a CADD phred score of 26.6. ClustalW alignment of TTC5 orthologues revealed that the missense variant pGly186 is evolutionary conserved among all species examined (data not shown) (CLUSTALW https://www.genome.jp/tools-bin/clustaw). Notably, the variants were not found in the control population referring to several public databases (dbSNP build150, gnomAD, ExAC, Exome Sequencing Project, 1000 Genomes). No other pathogenic or likely pathogenic variants which could explain the entire or partial phenotype were detected. To determine and corroborate putatively adverse functional effects of p.Gly186Val, we performed in silico 3D modeling (Project HOPE; Venselaar et al., 2010). The affected Glycine is located in the fifth TPR motif in the N-terminal tetratricopeptide repeat (TPR) domain which mediates protein–protein interactions and the assembly of multiprotein complexes (D'Andrea & Regan, 2003). TPR motif consists of 3–16 tandem repeats of 34 amino-acid residues. Sequence alignment of the TPR domains revealed a consensus sequence defined by a pattern of small and large amino acids. Although no position is entirely invariant, some residues are very conserved at only a few positions, for instance, Gly or Ala in position 8 of the repeat (D'Andrea & Regan, 2003), which is the position of Gly186 within the fifth TPR motif. Therefore, it is reasonable to hypothesize that the size difference between the wild-type and mutant residue could compromise the TPR domain structure. X-ray structure analysis corroborates this hypothesis, revealing that TPR adopts a helix-turn-helix arrangement, with adjacent TPR motifs packing in a parallel fashion, resulting in a spiral of repeating anti-parallel alpha-helices (D'Andrea & Regan, 2003). Substituting the very flexible glycine with another amino acid, like valine, could force the local backbone into an incorrect conformation and disturb the local structure.

The affected individual from family 2 presented a novel homozygous nonsense variant in the *TTC5* gene in exon 7 (NM_138376.2: c.771G>A; p.Trp257Ter), which passed segregation analysis according to a strict recessive mode of inheritance. The variant, predicted to be pathogenic following the ACMG guidelines and Varsome (Table S1), was not previously described in public databases. The premature stop codon introduced by the mutation is most likely to cause NMD, resulting in a complete loss of a functional gene product from both alleles. No other pathogenic or likely pathogenic variants which could explain the entire or partial phenotype were detected.

Exome sequencing of probands in unrelated families 3 and 5, the firstoriginating from Egypt and the second from Pakistan, identified in all affected individuals the homozygous nonsense variants in *TTC5* c.787C>T (NM_138376); p.(Arg263Ter), located in exon 7, that segregated with the phenotypes in the respective families. The variant was reported twice, in a heterozygous state in gnomAD (2/251092; allele frequency 0.000007965), predicted to be pathogenic following ACMG guidelines and Varsome (Table S1), and it was reported as disease-causing in two unrelated Egyptian families (5477 and 5543; Rasheed et al., 2021).

Affected individuals from family 4 had a novel homozygous nonsense variant in the *TTC5* gene (NM_138376.2: c.631_632insGTATG; p.Ala211GlyfsTer20) located in exon 7, predicted to be pathogenetic according to the ACMG guideline and Varsome (Table S1) and never described before in any public database, that segregated with the disease phenotype in the family. No other pathogenic or likely pathogenic variants which could explain the entire or partial phenotype were detected.

3.2 | Patients

The cohort consists of four males and three females, whose ages at the last evaluation ranged from 4 years and 6 months to 20 years. We provided a short description of each patient, reporting data not available in Tables 2–5 and Table S2. Table 2: overview of the core clinical features; Table 3: brain MRI findings; Table 4: craniofacial dysmorphic features; Table 5 growth parameters of the patients at birth and last examination; Table S2: Clinical features of all *TTC5* patients included in this study and previously published (Hu et al., 2019; Miyamoto et al., 2021; Rasheed et al., 2021).

3.3 | Clinical evolution

Patient 1 is the first child of unrelated Italian parents. He was born at term with microcephaly after a pregnancy characterized by intrauterine growth retardation (IUGR) (HP:0001511). From the second month of life, vomiting, feeding difficulties, and failure to thrive (HP:0001508) were observed. He presented with severe hypotonia (HP:0006829), excessive startle reactions, frequent diffuse spontaneous jerks, and bilateral cryptorchidism. At 10 months, the patient showed severe food avoidance and severe global developmental delay (HP:0011344) jointly with facial dysmorphic features.

At 12 months, the EEG documented an epileptic encephalopathy with abundant multifocal epileptic activity (HP:0010841). Myoclonic seizures (HP:0002123) and epileptic spasms (HP:0032842) were recorded on video EEG. Epileptic spasms responded to ACTH. Chronic treatment with several antiepileptic drugs was started, but "subtle" seizures (erratic myoclonias, hypomotor seizures, brief nystagmus episodes) persisted until the age of five. Metabolic analyses to investigate a possible inborn error of metabolism was performed and showed no abnormalities. Auditory brainstem response (ABR), visual

evoked potential (VEP), and nerve conduction study were normal. Because of persisting feeding problems, he underwent a gastrostomy at 21 months of age (HP:0011471). The evolution was characterized by a severe delay in motor milestones with pronounced lower limbs hypotrophy and spastic paresis (HP: 0002061) and unusual stereotyped manual movements.

At the last examination (10 years), the proband presented with microcephaly, short stature, and severe intellectual disability with verbal communication limited to a few words. After a seizure-free period, the epileptic encephalopathy relapsed with EEG abundant multifocal paroxysmal activity and with clinically evident sporadic myoclonic seizures in sleep.

Patient 2 is the second offspring of Iranian first cousins. The girl was born at term with microcephaly after a pregnancy characterized by IUGR (HP:0001511). Since birth, feeding difficulties and vomiting were observed; therefore, she was supported by a nasogastric tube. Craniofacial dysmorphic features were noted.

At the last examination (8.5 years), she showed severe intellectual disability, speech impairment (few single words), and autism-like behaviors such as self-mutilation (HP:0000742).

She presented with short stature, axial hypotonia (HP:0009062), brisk reflex, and contractures of the joints of the lower limbs (HP:0005750). She never achieved unassisted standing and walking ability.

Patient 3 is the first of two affected siblings from consanguineous Egyptian parents with unremarkable family history. He was born by cesarean delivery at 36 weeks of gestation due to premature membrane rupture after a pregnancy characterized by IUGR (HP:0001511). At the last examination (6 years), he had a severe ID, speech impairment with verbal communication limited to less than 10 words (HP:0002167) and facial dysmorphic features. He also showed microcephaly, short stature jointly with feeding difficulties, and being able to eat only soft food. In addition, he presented marked truncal hypotonia (HP:0008936), tetraparesis (HP:0001258) with hyperreflexia, and contracture (HP:0005750). He never achieved unassisted standing and walking ability.

Patient 4 is the younger sister of patient 3. She was born at term after a pregnancy characterized by IUGR (HP:0001511). At her last examination (4 years and 5 months), she showed a severe ID with absent speech (HP:0001344) and dysmorphic facial features. She presented microcephaly, short stature, truncal hypotonia (HP:0008936), and distal spastic paresis (HP:0002460), more severe in lower limbs (HP: 0002061). Like her brother, she never achieved unassisted standing and walking ability.

Patient 5 was the first of two affected siblings of Turkish first cousins. The boy was born at term with normal growth parameters. Feeding difficulties and vomiting were observed at 2 months (HP: 0008872), which persisted throughout life, and severe growth failure followed (HP: 0008850). From 4 months onwards, developmental delayed milestones with axial hypotonia (HP:0008936) and dystonic movements (HP:0001332) were detected. At 5 months, epileptic seizures occurred; the EEG showed paroxysmal and disorganized activity (HP:0011182) without typical hypsarrhythmia. Epilepsy did not

TABLE 2 Overview of the core clinical features of individuals with *TTC5* biallelic mutations

Patient	1	2	3	4	5	6	7	*TTC5* patients included in this study	*TTC5* patients previously reported (Hu et al., 2019; Miyamoto et al., 2021; Rasheed et al., 2021)	Total
Patient	1	2	3	4	5	6	7	7	12	19
Sex	M	F	M	F	M	M	F	3F:4M	4F:8M	7F:12M
Age at last examination	10 years	8 years 4 months	6 years	4 years 5 months	20 years	10 years	6 years	4 years 5 months 20 years	19 months–12 years	19 months–20 years
Growth retardation HP:0001510	+	+	+	+	+	−	+	6/7	8/12	74%
Short stature HP:0004322	+	+	+	+	+	−	+	5/6	8/12	72%
Feeding problems HP:0011968	+	+	+	−	+	+	+	6/7	1/1	87%
Microcephaly HP:0000252	+	+	+	+	−	−	+	5/7	7/10	63%
Speech impairment HP:0002167	+	+	+	+	+	+	+	7/7	12/12	100%
Hypotonia HP:0001252	+	+	+	+	+	+	+	7/7	7/9	88%
Standing inability	+	+	+	+	+	+	+	7/7	8/12	79%
Walking inability	+	+	+	+	+	+	+	7/7	8/8	100%
Developmental Delay/ID HP:0001263/ HP:0001249	+	+	+	+	+	+	+	7/7	12/12	100%
Mild HP:0001256									1/12	5%
Moderate HP:0002342									3/12	16%
Severe HP:0010864	+	+	+	+	+	+	+	7/7	8/12	79%
Seizures HP:0001250	+	−	−	−	+	+	+	4/7	1/12	26%
Abnormal brain MRI	+	+	+	+	+	+	+	7/7	9/9	100%
Cryptorchidism HP:0000028	+		−		+	+		3/4	2/5	60%

Note: Human phenotype ontology (HPO) terms are provided.

respond to several antiepileptic treatments in infancy; in childhood, valproate partially controlled the seizures that relapsed in adulthood. He started to sit independently at 4 years, but walking has never been achieved. The patient had severe scoliosis (HP:0002650), surgically corrected at 15 years. A severe ID, speech impairment with verbal communication limited to few words, facial dysmorphism, short stature, spastic tetraplegia (HP:0001258), and bilateral cryptorchidism were documented at 17 years. At this age, extensive diagnostic investigations (basic laboratory examinations, screening for lysosomal storage diseases, and enzyme testing) were normal like the nerve conduction studies. At the age of 20, the patient developed respiratory insufficiency and a significant weight gain probably due to

edema (>15 kg), for which antidiuretic therapy was started. ECG and echocardiography excluded cardiac insufficiency. He died at 26 years for unknown reasons.

Patient 6 is the younger brother of patient 5. He was born at 38 gestational weeks with growth parameters in the normal range. Neonatal feeding difficulties with frequent vomiting (HP:0008872) were reported. At 7 months, hypertonic stiffening of the extremities and concomitant lateral gaze deviation appeared monthly, therefore epileptic seizures were suspected but not confirmed. At that time the EEG during sleep was normal. At 9 years, the patient had a single focal seizure (HP:0007359). When he was 10, he presented severe ID with language limited to a few words, dysmorphic facial features, bilateral cryptorchidism, and spastic tetraplegia (HP:0002510). At the time,

TABLE 3 Brain MRI findings of the patients previously reported (1–12) and of the seven patients included in the current study (13–19) as reported by their physicians

	Patient	Cerebral atrophy	Ventriculomegaly (enlarged dysmorphic ventricles)	Cerebral cortex abnormalities	Callosal abnormalities	White matter abnormalities	Other
1	M9200013 III:2 (Hu et al., 2019)					Leukoencephalopathy HP:0002352	
2	M9200013 III:3 (Hu et al., 2019)				Agenesis corpus callosum HP:0001274	Supratentorial mild leukodystrophic pattern	
3	G033 II:1 (Hu et al., 2019)	NA	NA	NA	NA	NA	NA
4	RHDM-05 A (Rasheed et al., 2021)	Cerebral atrophy HP:0002059	–	–			
5	RHDM-05 B (Rasheed et al., 2021)	NA	NA	NA	NA	NA	NA
6	CW07 A (Rasheed et al., 2021)	Cerebral atrophy HP:0002059	Prominent anterior horns HP:0000245	Simplified gyral pattern HP:0009879	Corpus callosum atrophy HP:0007371		Dilated paranasal sinus HP:0000245 Distended straight sinus gliosis
7	CW07 B (Rasheed et al., 2021)	Cerebral atrophy HP:0002059	Ventriculomegaly of the third and lateral ventricles HP:0002119	Simplified gyral pattern HP:0009879	Corpus callosum atrophy HP:0007371		Enlarged paranasal HP:0000245 and distended straight sinus, prominent sylvian fissures HP:0100952
8	5543 (Rasheed et al., 2021)	Cerebral atrophy HP:0002059	Dilated lateral ventricles HP:0002119	Simplified gyral pattern HP:0009879	Corpus callosum hypoplasia HP:0002079	White matter abnormalities around the occipital horn HP:0007052	
9	5377 (Rasheed et al., 2021)	Central and cortical atrophy HP:0002120	Dilated lateral ventricles HP:0002119	Abnormal gyri HP:0002536	Thin corpus callosum HP:0033725		
10	6772 A (Rasheed et al., 2021)	Cortical atrophy HP:0002120	Dilated lateral ventricles HP:0002119	Abnormal gyri HP:0002536	Thin corpus callosum HP:0033725		
11	6772 B (Rasheed et al., 2021)	Cerebral atrophy HP:0002059	Dilated lateral and third ventricles HP:0002119	Simplified gyral pattern HP:0009879	Hypoplastic corpus callosum HP:0002079		
12	Pat 1 (Miyamoto et al., 2021)			Simplified gyral pattern HP:0009879	Thin corpus callosum HP:0033725	Mildly delayed myelination of frontal subcortical white matter high-intensity signal on T2WI and FLAIR at deep white matter	At 1 month undetectable anterior limb of the internal capsule At 22 months anterior limb of internal capsule "weak"

(Continues)

TABLE 3 (Continued)

Patient	Cerebral atrophy	Ventriculomegaly (enlarged dysmorphic ventricles)	Cerebral cortex abnormalities	Callosal abnormalities	White matter abnormalities	Other
13 Patient 1 (current study)		Mild ventriculomegaly In the frontal area HP:0006956 Square aspect of the occipital horns HP:0002118	Abnormal gyri HP:0002536 Simplification of the parietal gyration bilaterally Along the lateral sulcus HP:0009879 Cortical thickening of the bilateral supramarginal gyrus HP:0006891	Corpus callosum atrophy HP:0007371	Supratentorial with matter atrophy HP:0012762	
14 Patient 2 (current study)			Microgyria in CT (no MRI)			
15 Patient 3 (current study)	Cerebral atrophy HP:0002059					
16 Patient 4 (current study)	Mild cerebral atrophy HP:0002059				Mild periventricular leukomalacia HP:0006970	
17 Patient 5 (current study)	Cerebral atrophy HP:0002059	Enlarged ventricles HP:0002119		Corpus callosum atrophy HP:0007371	Supratentorial white matter atrophy HP:0012762	
18 Patient 6 (current study)	Cerebral atrophy HP:0002059	Enlarged ventricles most in the frontal lateral HP:0002119	Bilateral perisylvian and postcentral polymicrogyria HP:0012650	Corpus callosum atrophy HP:0007371		
19 Patient 7 (current study)		Dysmorphic ventricles HP:0002118			Reduced white matter volume HP:0012762 Reduced myelination HP:0012448	Right sided cortical dysplasia HP:0002539

Note: Human phenotype ontology (HPO) terms are provided. Patient 5 and Patient 6 (current study): MR spectroscopy showed a decreased in all metabolites except choline that was in normal concentration.

TABLE 4 Craniofacial dysmorphic features of patients with *TTC5* variants included in this study

Main craniofacial features	Number of patients
Prominent forehead (HP:0011220)	6/7
Broad arched eyebrows (HP:0002553)	7/7
Hypertelorism (HP:000031)	7/7
Upslanted palpebral fissure (HP:0000582)	4/7
Downslanted palpebral fissures (HP:0000494)	3/7
Strabismus (HP:0000486)	4/7
Proptosis (HP:0000520)	4/7
Short nose (HP:0003196)	7/7
Depressed nasal bridge (HP:0005280)	7/7
Bulbous tip of nose (HP:0005274)	7/7
Anteverted nares (HP:0000463)	5/7
Long philtrum (HP:0000343)	6/7
Full cheeks (HP:0000293)	7/7
Downturned mouth (HP:0002714)	7/7

Note: Human phenotype ontology (HPO) terms are provided.

mild peripheral edema was noted. All metabolic investigations were normal. He never achieved the ability to stand and walk unassisted.

Patient 7 is a girl born of Pakistani first cousins. Pregnancy was complicated by oligohydramnios (HP:0001562) and IUGR (HP:0001511). She was delivered by cesarean section at 38 weeks of gestation, with reduced auxologic parameters. At 2 months, she developed seizures, possibly due to hypocalcemia. At 3 years, she presented microcephaly, severe global developmental delay (HP:0011344), and speech impairment with communication limited to a few words. She showed axial hypotonia (HP:0008936), dystonic posturing of the hand (HP:0031969), and hypertonia with brisk reflexes of the lower limbs (HP:0002061). She did not achieve unassisted standing and walking ability. At 4 years of age, hypercalcemic hyperparathyroidism was diagnosed. At 4.5 years, a pelvic ganglion-euroblastoma was incidentally detected during an ultrasound assessment for nephrocalcinosis.

4 | DISCUSSION

In 2019, Hu and colleagues identified *TTC5* as a candidate gene for autosomal recessive ID (ARID) in two unrelated consanguineous families (Hu et al., 2019). Two years later, Rasheed et al., reporting seven additional patients, identified the core clinical features, including severe speech impairment, cerebral atrophy, and hypotonia, to prioritize this syndrome for diagnosis. Defining *TTC5* disorder as an IDs associated syndrome, the authors draw attention to the possible underlying molecular mechanism, namely reduced p300 co-activator complex activity, and compare the phenotype with RSTS2 syndrome, caused by *EP300* variants, suggesting that a shared pathomechanism could result in clinical similarities between the two conditions (Rasheed et al., 2021). On the other hand, the same authors suggested

that the differences in the clinical presentation and the severity between the two conditions could be attributed to additional TTC5 functions unrelated to the p300 network, including tubulin autoregulation. More recently, Miyamoto reported a boy with biallelic frameshift variants in *TTC5*, providing functional data and brain MRI findings to suggest a link between TTC5-related brain malformation and tubulinopathies (Miyamoto et al., 2021).

The present study provides the molecular spectrum, the clinical evolution, and the deep reverse phenotyping of seven new TTC5 patients. The previously emerged clinical phenotype is confirmed, and new elements are added to delineate a recognizable very severe neurodevelopmental syndrome in the broad spectrum of NDDs (Tables 2–5 and Table S2). The hypothesis that alterations in different genes could converge functionally to the same molecular effect (alteration opening/closing chromatin/epigenetic modification) to determine overlapping clinical conditions prompted us to review the MHKH1 patients (Table S3).

4.0.1 | Clinical evolution

In most cases, delivery occurred at term, but a global development delay starting from early infancy was reported; general hypotonia evolving toward axial hypotonia and spasticity mainly in the lower limbs characterized the evolution of motor development in all individuals. At the last examination, none of the patients acquired the ability to stand and walk independently. The significant impairment of cognitive and language function was consistent with the features of previously reported patients and confirmed the severity of the disorder. Psychomotor evolution was generally less severe in MKHK1 syndrome than in TTC5 patients. Cognitive and language function impairment was reported in all MKHK1 patients but with a more variable degree of severity; insufficient data were provided concerning the presence of hypotonia; a delay in the ability to walk independently was observed, but it was eventually obtained (Table S3).

4.0.2 | Brain malformations

All *TTC5* patients described in the literature and all individuals in this study showed abnormal brain MRI findings (Table 3). In particular, a simplified gyral pattern was described in six out of eight patients (Hu et al., 2019; Miyamoto et al., 2021; Rasheed et al., 2021). Malformations of cortical development (MCDs; microgyria, polymicrogyria, abnormal gyri, simplification of gyration, cortical thickening) were reported in three out of seven of our patients. Moreover, in addition to the cortical phenotype, extra-cortical brain features are also reported in *TTC5* patients (Table 3). These features are consistent with the imaging pattern of brain malformations associated with tubulinopathies (Romaniello et al., 2018).

In this regard, TTC5 mediates autoregulation of tubulin via its mRNA degradation, binding the ribosome through the OB domain and making some critical protein–protein contact with amino acids located

TABLE 5 Growth parameters of *TTC5* patients reported in this study

Patient	1	2	3	4	5	6	7
Gender	M	F	M	F	M	M	F
Gestational age	term	40 weeks	36 weeks	term	39 weeks	38 weeks	38 weeks 6 days
Growth parameters at birth							
OFC (cm)	30.5(−2.8 SD)	29 (−3.9 SD)	NA	NA	34 (−0.8 SD)	33 (−1.2 SD)	NA
Length (cm)	44 (−2.8 SD)	43 (−2.9 SD)	NA	NA	49 (−0.4 SD)	49 (−0.4 SD)	NA
Weight (g)	2460 (−3.2 SD)	1600 (−3.5 SD)	1700 (−2.9 SD)	2000 (−2.7 SD)	3150 (−0.6 SD)	2860 (−1.1 SD)	2360 (−2.0 SD)
Age at last examination	10 years	8 years 4 months	6 years	4 years 5 months	20 years	10 years	6 years
Growth parameters at last examination							
OFC (cm)	49 (−3.0 SD)	44 (−6.3 SD)	47.2 (−2.7 SD)	46.5 (−2.3 SD)	54 (−1.8 SD) (at 17 years)	54 (+0.8 SD)	44.8 (−4.9 SD)
Height (cm)	118 (−3.2 SD)	100 (−5.0 SD)	93 (−5.4 SD)	82 (−4.9 SD)	150 (−3.7 SD) (at 17 years)	138 (−0.1 SD)	NA
Weight (kg)	19.8 (−2.9 SD)	11 (−4.5 SD)	11 (−4.6 SD)	9 (−4.3 SD)	40 (−4.9 SD) (at 17 years)	37.1 (+0.5 SD)	NA

Abbreviation: OFC, occipital–frontal circumference.

in the fifth TRP motif of the tetratricopeptide domain. Recently, Miyamoto provided a detailed neuroradiological description of a Japanese boy with *TTC5* mutations, and he showed that reduced TTC5 protein level could induce a decrease of β3 tubulin, a neuronal-specific isotype. Since the decreased level of β3 tubulin could lead to an aberrant cell cycle, the authors suggested a possible link role of TTC5 in cell cycle regulation; however, the author stressed the necessity of new experiments with knockout neural cells or mice to provide additional evidence about the functional role of TTC5 and mutation related disorder in the pathomechanism (Miyamoto et al., 2021). Functionally, the frameshift and stop mutations we found in *TTC5* likely cause NMD, leading to a decreased amount of protein available. Experimental outcomes corroborated this hypothesis (Rasheed et al., 2021). Decreased TTC5 protein levels could determine a reduced tubulin autoregulation rate, whereas the missense mutation affecting the fifth TRP motif very likely results in altered protein–protein interactions.

4.0.3 | Epilepsy

In our series, patients 1, 5, and 6 presented spontaneous seizures. Patients 1 and 5 had epileptic spasms without a typical hypsarrhythmic EEG pattern. Patient 7 presented seizures at 2 months of life, possibly due to hypocalcemia. In the Rasheed series, only one patient (patient 5377 in Family 4) at 2 years developed epilepsy with tonic and myoclonic seizures and then controlled with antiepileptic medications (Rasheed et al., 2021). The author did not rule out the possibility that *TTC5* variants could contribute to epilepsy. Epilepsy is usually present, with a wide range of severity and no specific pattern in tubulinopathies. In this regard, the accurate analysis of the EEG in wakefulness and sleep allowed the detection of significant abnormalities of the background activity in all the patients reported by Romaniello et al. (2019). The EEG

features of *TTC5* patients were not reported in the Rasheed series; however, interestingly, Miyamoto described an abnormal EEG with no epileptic discharge or apparent seizures in his patient (Miyamoto et al., 2021). Concerning the clinical diagnosis of epilepsy and its entry, among other features characterizing the disorder, it could be argued that seizures can be subtle and difficult to recognize, especially in patients with severe cognitive and motor impairment.

4.0.4 | Pre- and post-natal growth retardation, short stature

Most of the patients of our series (except for two siblings) presented an IUGR; the growth failure continued postnatally (Table 5 and Table S2), as in the case reported by Miyamoto and possibly attributed to a growth hormone deficiency by the author (Miyamoto et al., 2021). The feeding difficulties, including vomiting and food avoidance, described in almost all of our patients (1, 2, 3, 5, 6, and 7) could be related to swallowing and chewing difficulties and the severity of neurological impairment (Table S2). Moreover, a specific TTC5 role in development and growth could also be hypothesized.

In all but one case so far described, the mutations identified are either frameshifts, stop codon, or a missense change affecting exons coding for the OB domain or located in the fifth and sixth TRP motifs, supporting the critical role of those regions. The TRP domain in TTC5 allowed the binding of different components of the p300 complex in the nucleus (Demonacos et al., 2001), interacting directly with p300. CREB-binding protein, a p300 paralog, is also an important coactivator in the p300 transcriptional regulatory network. Two regions in p300 are responsible for binding TTC5, including aa 1572–1921, encoded by exons 30 and 31 of *EP300* gene (Demonacos et al., 2001).

Only recently, heterozygous mutations in these exons and in the homologous region of the CREB-binding protein *(CREBBP)* gene were

found responsible for Menke–Hennekam syndrome 1 and 2 (MKHK1 and 2; Angius et al., 2019; Banka et al., 2019; Menke et al., 2016, 2018; Nishi et al., 2022; Wang et al., 2021). The main MKHK1 characteristics are psychomotor delay, variable impairment of intellectual disability (ID), feeding difficulties, autistic behavior, hearing impairment, short stature, facial dysmorphisms, and microcephaly. Notably, in 87% and 45% of MKHK1 patients, feeding problems and short stature were described (Table S3). The patient reported by Angius et al. (2019) and all the three patients described by Banka et al. (2019) had feeding difficulties and reduced growth parameters. Moreover, five of six patients recently observed by Nishi and colleagues had prenatal growth failure, and four had postnatal growth failure (Nishi et al., 2022). Given the overlapping clinical features between TTC5 and MKHK1 patients and this cell-biological knowledge, it is reasonable to speculate that TTC5, p300, and CREBBP could affect the function of a common molecular pathway. In this regard, it has been shown that the p300 activator complex mediates p53 transcriptional response to cell stress (Demonacos et al., 2001). In particular, the lack of nutrients results in the enhanced transcription of Pten, TSC2, and AMPK, blocking the functioning of the IGF-1/mTor pathways leading to a decrease in cell growth (Feng, 2010).

4.0.5 | Facial dysmorphisms

The facial dysmorphisms in TTC5 patients are generally not specific, but their association in these individuals characterizes a common facial gestalt (Table 4). Moreover, some of these features overlap with the clinical facial characteristics of MKHK1 syndrome patients, including a prominent forehead, highly arched eyebrows, up-slanted or down-slanted palpebral fissures, depressed nasal bridge, short nose, anteverted nares, long philtrum, and full cheeks.

5 | CONCLUSION

We described seven affected individuals from five unrelated families with homozygous and compound heterozygous variants in the TTC5 gene. In total 19 patients have been so far described. Two of them were offspring of non-consanguineous parents and had compound heterozygous TTC5 variants.

The detailed reverse phenotyping of our cases and the comparison with the published ones allowed us to underline some recurrent characteristics, in particular, (1) the severity of the condition both for neurodevelopment and for intellectual disability, (2) the inability to reach the stand position and to walk, (3) the severe language disorder, (4) the brain malformations, (5) the severe growth retardation, (6) cryptorchidism and (7) the common facial gestalt.

Epilepsy was present in about a quarter of patients with TTC5-related disorder and in the same proportion of MKHK1 patients. It would be desirable to obtain clinical neurophysiological and neuroradiological information in a larger number of patients to study and compare in detail this feature. The comparison with

MKHK1 patients highlighted an overlapping of clinical features, particularly the feeding problems, pre- and post-natal growth retardation, the severity of language impairment, and facial features. These observations are intended to be a background stimulus to promote functional studies to verify the hypothesis of the causative role of a disrupted molecular pathway involving p300 and its influence in determining shared phenotype characteristics. Molecular understanding of the disease mechanism and more specific clinical data derived from targeted interpretation of neuroimaging and electroclinical assessment are also needed to confirm the link of TTC5 with tubulinopathies in the reversal phenotype approach.

ORCID

Luciana Musante https://orcid.org/0000-0002-2742-1484
Flavio Faletra https://orcid.org/0000-0003-1483-3612
Hoda Tomoum https://orcid.org/0000-0002-7781-7532
Paria Najarzadeh Torbati https://orcid.org/0000-0001-7583-4614
Jutta Gärtner https://orcid.org/0000-0003-4108-7109
Susann Diegmann https://orcid.org/0000-0001-9134-6303

Mehran Beiraghi Toosi https://orcid.org/0000-0002-0569-1117

Farah Ashrafzadeh https://orcid.org/0000-0002-8345-5646

Ehsan Ghayoor Karimiani https://orcid.org/0000-0003-3858-7073

David Murphy https://orcid.org/0000-0002-3771-3800

Flora Maria Murru https://orcid.org/0000-0001-8954-8889

Caterina Zanus https://orcid.org/0000-0001-7235-4965

Andrea Magnolato https://orcid.org/0000-0002-5099-6526

Agnese Feresin https://orcid.org/0000-0002-4187-6282

Giorgia Girotto https://orcid.org/0000-0003-4507-6589

Paolo Gasparini https://orcid.org/0000-0002-0859-0856

Paola Costa https://orcid.org/0000-0003-0546-6005

Marco Carrozzi https://orcid.org/0000-0001-6282-4417

REFERENCES

Abramov, D., Guiberson, N. G. L., & Burré, J. (2021). STXBP1 encephalopathies: Clinical spectrum, disease mechanisms, and therapeutic strategies. *Journal of Neurochemistry*, *157*(2), 165–178. https://doi.org/10.1111/jnc.15120

Adzhubei, I., Jordan, D. M., & Sunyaev, S. R. (2013). Predicting functional effect of human missense mutations using PolyPhen-2. *Current Protocols in Human Genetics*, *Chapter 7*, Unit 7.20. https://doi.org/10.1002/0471142905.hg0720s76

Angius, A., Uva, P., Oppo, M., Persico, I., Onano, S., Olla, S., Pes, V., Perria, C., Cuccuru, G., Atzeni, R., Serra, G., Cucca, F., Sotgiu, S., Hennekam, R. C., & Crisponi, L. (2019). Confirmation of a new phenotype in an individual with a variant in the last part of exon 30 of CREBBP. *American Journal of Medical Genetics Part A*, *179*(4), 634–638. https://doi.org/10.1002/ajmg.a.61052

Banka, S., Sayer, R., Breen, C., Barton, S., Pavaine, J., Sheppard, S. E., Bedoukian, E., Skraban, C., Cuddapah, V. A., & Clayton-Smith, J. (2019). Genotype-phenotype specificity in Menke-Hennekam syndrome caused by missense variants in exon 30 or 31 of CREBBP. *American Journal of Medical Genetics. Part A*, *179*(6), 1058–1062. https://doi.org/10.1002/ajmg.a.61131

Bauer, P., Kandaswamy, K. K., Weiss, M. E. R., Paknia, O., Werber, M., Bertoli-Avella, A. M., Yüksel, Z., Bochinska, M., Oprea, G. E., Kishore, S., Weckesser, V., Karges, E., & Rolfs, A. (2019). Development of an evidence-based algorithm that optimizes sensitivity and specificity in ES-based diagnostics of a clinically heterogeneous patient population. *Genetics in Medicine*, *21*(1), 53–61. https://doi.org/10.1038/s41436-018-0016-6

D'Andrea, L. D., & Regan, L. (2003). TPR proteins: The versatile helix. *Trends in Biochemical Sciences*, *28*(12), 655–662. https://doi.org/10.1016/j.tibs.2003.10.007

Davies, L., Paraskevopoulou, E., Sadeq, M., Symeou, C., Pantelidou, C., Demonacos, C., & Krstic-Demonacos, M. (2011). Regulation of glucocorticoid receptor activity by a stress responsive transcriptional cofactor. *Molecular Endocrinology (Baltimore, MD)*, *25*(1), 58–71. https://doi.org/10.1210/me.2010-0212

de Goede, C., Yue, W. W., Yan, G., Ariyaratnam, S., Chandler, K. E., Downes, L., Khan, N., Mohan, M., Lowe, M., & Banka, S. (2016). Role of reverse phenotyping in interpretation of next generation sequencing data and a review of INPP5E related disorders. *European Journal of Paediatric Neurology*, *20*(2), 286–295. https://doi.org/10.1016/j.ejpn.2015.11.012

Deciphering Developmental Disorders Study. (2017). Prevalence and architecture of de novo mutations in developmental disorders. *Nature*, *542*(7642), 433–438. https://doi.org/10.1038/nature21062

Demonacos, C., Krstic-Demonacos, M., & La Thangue, N. B. (2001). A TPR motif cofactor contributes to p300 activity in the p53 response. *Molecular Cell*, *8*(1), 71–84. https://doi.org/10.1016/s1097-2765(01)00277-5

Dent, E. W. (2017). Of microtubules and memory: Implications for microtubule dynamics in dendrites and spines. *Molecular Biology of the Cell*, *28*(1), 1–8. https://doi.org/10.1091/mbc.E15-11-0769

Efthymiou, S., Dutra-Clarke, M., Maroofian, R., Kaiyrzhanov, R., Scala, M., Reza Alvi, J., Sultan, T., Christoforou, M., Tuyet Mai Nguyen, T., Mankad, K., Vona, B., Rad, A., Striano, P., Salpietro, V., Guillen Sacoto, M. J., Zaki, M. S., Gleeson, J. G., Campeau, P. M., Russell, B. E., & Houlden, H. (2021). Expanding the phenotype of PIGS-associated early onset epileptic developmental encephalopathy. *Epilepsia*, *62*(2), e35–e41. https://doi.org/10.1111/epi.16801

Feng, Z. (2010). P53 regulation of the IGF-1/AKT/mTOR pathways and the endosomal compartment. *Cold Spring Harbor Perspectives in Biology*, *2*(2), a001057. https://doi.org/10.1101/cshperspect.a001057

Firth, H. V., Wright, C. F., & DDD Study. (2011). The deciphering developmental disorders (DDD) study. *Developmental Medicine and Child Neurology*, *53*(8), 702–703. https://doi.org/10.1111/j.1469-8749.2011.04032.x

Hu, H., Kahrizi, K., Musante, L., Fattahi, Z., Herwig, R., Hosseini, M., Oppitz, C., Abedini, S. S., Suckow, V., Larti, F., Beheshtian, M., Lipkowitz, B., Akhtarkhavari, T., Mehvari, S., Otto, S., Mohseni, M., Arzhangi, S., Jamali, P., Mojahedi, F., ... Najmabadi, H. (2019). Genetics of intellectual disability in consanguineous families. *Molecular Psychiatry*, *24*(7), 1027–1039. https://doi.org/10.1038/s41380-017-0012-2

Jian, X., Boerwinkle, E., & Liu, X. (2014). In silico prediction of splice-altering single nucleotide variants in the human genome. *Nucleic Acids Research*, *42*(22), 13534–13544. https://doi.org/10.1093/nar/gku1206

Kircher, M., Witten, D. M., Jain, P., O'Roak, B. J., Cooper, G. M., & Shendure, J. (2014). A general framework for estimating the relative pathogenicity of human genetic variants. *Nature Genetics*, *46*(3), 310–315. https://doi.org/10.1038/ng.2892

Köhler, S., Gargano, M., Matentzoglu, N., Carmody, L. C., Lewis-Smith, D., Vasilevsky, N. A., Danis, D., Balagura, G., Baynam, G., Brower, A. M., Callahan, T. J., Chute, C. G., Est, J. L., Galer, P. D., Ganesan, S., Griese, M., Haimel, M., Pazmandi, J., Hanauer, M., ... Robinson, P. N. (2021). The human phenotype ontology in 2021. *Nucleic Acids Research*, *49*(D1), D1207–D1217. https://doi.org/10.1093/nar/gkaa1043

Limongelli, I., Marini, S., & Bellazzi, R. (2015). PaPI: Pseudo amino acid composition to score human protein-coding variants. *BMC Bioinformatics*, *16*, 123. https://doi.org/10.1186/s12859-015-0554-8

Lin, Z., Gasic, I., Chandrasekaran, V., Peters, N., Shao, S., Mitchison, T. J., & Hegde, R. S. (2020). TTC5 mediates autoregulation of tubulin via mRNA degradation. *Science (New York, N.Y.)*, *367*(6473), 100–104. https://doi.org/10.1126/science.aaz4352

Menke, L. A., DDD study, Gardeitchik, T., Hammond, P., Heimdal, K. R., Houge, G., Hufnagel, S. B., Ji, J., Johansson, S., Kant, S. G., Kinning, E., Leon, E. L., Newbury-Ecob, R., Paolacci, S., Pfundt, R., Ragge, N. K., Rinne, T., Ruivenkamp, C., Saitta, S. C., ... Hennekam, R. C. (2018). Further delineation of an entity caused by CREBBP and EP300 mutations but not resembling Rubinstein-Taybi syndrome. *American Journal of Medical Genetics. Part A*, *176*(4), 862–876. https://doi.org/10.1002/ajmg.a.38626

Menke, L. A., van Belzen, M. J., Alders, M., Cristofoli, F., Study, D. D. D., Ehmke, N., Fergelot, P., Foster, A., Gerkes, E. H., Hoffer, M. J. V., Horn, D., Kant, S. G., Lacombe, D., Leon, E., Maas, S. M., Melis, D., Muto, V., Park, S.-M., Peeters, H., ... Hennekam, R. C. M. (2016). CREBBP mutations in individuals without Rubinstein-Taybi syndrome phenotype. *American Journal of Medical Genetics. Part A*, *170*(10), 2681–2693. https://doi.org/10.1002/ajmg.a.37800

Miyamoto, S., Kato, M., Sugiyama, K., Horiguchi, R., Nakashima, M., Aoto, K., Mutoh, H., & Saitsu, H. (2021). A boy with biallelic frameshift variants in TTC5 and brain malformation resembling tubulinopathies. *Journal of Human Genetics*, *66*(12), 1189–1192. https://doi.org/10.1038/s10038-021-00953-7

Musante, L., Costa, P., Zanus, C., Faletra, F., Murru, F. M., Bianco, A. M., La Bianca, M., Ragusa, G., Athanasakis, E., d'Adamo, A. P., Carrozzi, M., & Gasparini, P. (2022). The genetic diagnosis of Ultrarare DEEs: An ongoing challenge. *Genes*, *13*(3), 500. https://doi.org/10.3390/genes13030500

Nishi, E., Takenouchi, T., Miya, F., Uehara, T., Yanagi, K., Hasegawa, Y., Ueda, K., Mizuno, S., Kaname, T., Kosaki, K., & Okamoto, N. (2022). The novel and recurrent variants in exon 31 of CREBBP in Japanese patients with Menke-Hennekam syndrome. *American Journal of Medical Genetics. Part A*, *188*(2), 446–453. https://doi.org/10.1002/ajmg.a.62533

Quang, D., Chen, Y., & Xie, X. (2015). DANN: A deep learning approach for annotating the pathogenicity of genetic variants. *Bioinformatics (Oxford, England)*, *31*(5), 761–763. https://doi.org/10.1093/bioinformatics/btu703

Rasheed, A., Gumus, E., Zaki, M., Johnson, K., Manzoor, H., LaForce, G., Ross, D., McEvoy-Venneri, J., Stanley, V., Lee, S., Virani, A., Ben-Omran, T., Gleeson, J. G., Naz, S., & Schaffer, A. (2021). Bi-allelic TTC5 variants cause delayed developmental milestones and intellectual disability. *Journal of Medical Genetics*, *58*(4), 237–246. https://doi.org/10.1136/jmedgenet-2020-106849

Richards, S., Aziz, N., Bale, S., Bick, D., Das, S., Gastier-Foster, J., Grody, W. W., Hegde, M., Lyon, E., Spector, E., Voelkerding, K., Rehm, H. L., & ACMG Laboratory Quality Assurance Committee. (2015). Standards and guidelines for the interpretation of sequence variants: A joint consensus recommendation of the American College of Medical Genetics and Genomics and the Association for Molecular Pathology. *Genetics in Medicine*, *17*(5), 405–424. https://doi.org/10.1038/gim.2015.30

Romaniello, R., Arrigoni, F., Fry, A. E., Bassi, M. T., Rees, M. I., Borgatti, R., Pilz, D. T., & Cushion, T. D. (2018). Tubulin genes and malformations of cortical development. *European Journal of Medical Genetics*, *61*(12), 744–754. https://doi.org/10.1016/j.ejmg.2018.07.012

Romaniello, R., Zucca, C., Arrigoni, F., Bonanni, P., Panzeri, E., Bassi, M. T., & Borgatti, R. (2019). Epilepsy in tubulinopathy: Personal series and literature review. *Cell*, *8*(7), E669. https://doi.org/10.3390/cells8070669

Saunders, H. A. J., Johnson-Schlitz, D. M., Jenkins, B. V., Volkert, P. J., Yang, S. Z., & Wildonger, J. (2022). Acetylated α-tubulin K394 regulates microtubule stability to shape the growth of axon terminals. *Current Biology*, *32*(3), 614–630.e5. https://doi.org/10.1016/j.cub.2021.12.012

Sim, N.-L., Kumar, P., Hu, J., Henikoff, S., Schneider, G., & Ng, P. C. (2012). SIFT web server: Predicting effects of amino acid substitutions on proteins. *Nucleic Acids Research*, *40*, W452–W457. https://doi.org/10.1093/nar/gks539

Sobreira, N., Schiettecatte, F., Valle, D., & Hamosh, A. (2015). GeneMatcher: A matching tool for connecting investigators with an interest in the same gene. *Human Mutation*, *36*(10), 928–930. https://doi.org/10.1002/humu.22844

Stessman, H. A. F., Xiong, B., Coe, B. P., Wang, T., Hoekzema, K., Fenckova, M., Kvarnung, M., Gerdts, J., Trinh, S., Cosemans, N., Vives, L., Lin, J., Turner, T. N., Santen, G., Ruivenkamp, C., Kriek, M., van Haeringen, A., Aten, E., Friend, K., ... Eichler, E. E. (2017). Targeted sequencing identifies 91 neurodevelopmental-disorder risk genes with autism and developmental-disability biases. *Nature Genetics*, *49*(4), 515–526. https://doi.org/10.1038/ng.3792

Uliana, V., & Percesepe, A. (2016). Reverse phenotyping comes of age. *Molecular Genetics and Metabolism*, *118*(4), 230–231. https://doi.org/10.1016/j.ymgme.2016.05.010

Van Gils, J., Magdinier, F., Fergelot, P., & Lacombe, D. (2021). Rubinstein-Taybi syndrome: A model of epigenetic disorder. *Genes*, *12*(7), 968. https://doi.org/10.3390/genes12070968

Venselaar, H., Te Beek, T. A. H., Kuipers, R. K. P., Hekkelman, M. L., & Vriend, G. (2010). Protein structure analysis of mutations causing inheritable diseases. An e-science approach with life scientist friendly interfaces. *BMC Bioinformatics*, *11*, 548. https://doi.org/10.1186/1471-2105-11-548

Vulto-van Silfhout, A. T., Gilissen, C., Goeman, J. J., Jansen, S., van Amen-Hellebrekers, C. J. M., van Bon, B. W. M., Koolen, D. A., Sistermans, E. A., Brunner, H. G., de Brouwer, A. P. M., & de Vries, B. B. A. (2017). Quantification of phenotype information aids the identification of novel disease genes. *Human Mutation*, *38*(5), 594–599. https://doi.org/10.1002/humu.23176

Wang, Q., Xu, W., Liu, Y., & Yuan, H. (2021). A novel CREBBP in-frame deletion variant in a Chinese girl with atypical Rubinstein-Taybi syndrome phenotypes. *Journal of Molecular Neuroscience*, *71*(3), 607–612. https://doi.org/10.1007/s12031-020-01681-x

Weng, P. L., Majmundar, A. J., Khan, K., Lim, T. Y., Shril, S., Jin, G., Musgrove, J., Wang, M., Ahram, D. F., Aggarwal, V. S., Bier, L. E., Heinzen, E. L., Onuchic-Whitford, A. C., Mann, N., Buerger, F., Schneider, R., Deutsch, K., Kitzler, T. M., Klämbt, V., ... Sanna-Cherchi, S. (2021). De novo TRIM8 variants impair its protein localization to nuclear bodies and cause developmental delay, epilepsy, and focal segmental glomerulosclerosis. *American Journal of Human Genetics*, *108*(2), 357–367. https://doi.org/10.1016/j.ajhg.2021.01.008

Xiong, Y., Wang, L., Deng, W., Wang, J., & Shi, T. (2013). Human TTC5, a novel tetratricopeptide repeat domain containing gene, activates p53 and inhibits AP-1 pathway. *Molecular Biology Reports*, *40*(11), 6183–6188. https://doi.org/10.1007/s11033-013-2729-6

SUPPORTING INFORMATION

Additional supporting information may be found in the online version of the article at the publisher's website.